

# Genome-wide Orchestration of Cardiac Functions by the Orphan Nuclear Receptors $ERR\alpha$ and $\gamma$

Catherine R. Dufour,<sup>1</sup> Brian J. Wilson,<sup>1</sup> Janice M. Huss,<sup>2</sup> Daniel P. Kelly,<sup>3</sup> William A. Alaynick,<sup>4</sup> Michael Downes,<sup>4</sup> Ronald M. Evans,<sup>4</sup> Mathieu Blanchette,<sup>5</sup> and Vincent Giguère<sup>1,6,\*</sup>

<sup>1</sup> Molecular Oncology Group, McGill University Health Centre, Montréal, Québec H3A 1A1, Canada

<sup>2</sup> Department of Gene Regulation and Discovery, City of Hope, Duarte, CA 91010, USA

<sup>3</sup> Center for Cardiovascular Research and Department of Medicine, Washington University School of Medicine, St. Louis, MO 63110, USA

<sup>4</sup> Howard Hughes Medical Institute and Gene Expression Laboratory, The Salk Institute for Biological Studies, La Jolla, CA 92037, USA

<sup>5</sup> McGill Centre for Bioinformatics, Montréal, Québec H3A 2B4, Canada

<sup>6</sup> Departments of Biochemistry, Medicine, and Oncology, McGill University, Montréal, Québec H3A 1A1, Canada

\*Correspondence: [vincent.giguere@mcgill.ca](mailto:vincent.giguere@mcgill.ca)

DOI 10.1016/j.cmet.2007.03.007

## SUMMARY

Orphan nuclear receptor  $ERR\alpha$  (NR3B1) is recognized as a key regulator of mitochondrial biogenesis, but it is not known whether  $ERR\alpha$  and other ERR isoforms play a broader role in cardiac energetics and function. We used genome-wide location analysis and expression profiling to appraise the role of  $ERR\alpha$  and  $\gamma$  (NR3B3) in the adult heart. Our data indicate that the two receptors, acting as nonobligatory heterodimers, target a common set of promoters involved in the uptake of energy substrates, production and transport of ATP across the mitochondrial membranes, and intracellular fuel sensing, as well as  $Ca^{2+}$  handling and contractile work. Motif-finding algorithms assisted by functional studies indicated that ERR target promoters are enriched for NRF-1, CREB, and STAT3 binding sites. Our study thus reveals that the ERRs orchestrate a comprehensive cardiac transcriptional program and further suggests that modulation of ERR activities could be used to manage cardiomyopathies.

## INTRODUCTION

To function as an efficient and reliable pump and remain healthy, the heart must relentlessly produce enough ATP to sustain intracellular  $Ca^{2+}$  homeostasis for contraction. The heart must be able to switch between carbohydrates and fatty acids (FAs) as sources of energy in response to the physiological status of the organism and to gauge the cellular energy content of cardiomyocytes (Taegtmeyer et al., 2004). This metabolic plasticity is mediated by allosteric controls and phosphorylation cascades for short-term adjustments as well as gene regulatory mechanisms that involve coordinated expression changes in

metabolic pathway genes for enduring alterations. This regulatory system requires the parallel regulation of a network of genes encoding proteins implicated in FA and glucose uptake, delivery of intermediates into the mitochondria, FA  $\beta$ -oxidation (FAO), and pyruvate oxidation complexes, as well as the shared oxidative pathways of tricarboxylic acid (TCA), the electron transport complex (ETC), and oxidative phosphorylation (OXPHOS). Coordinately regulated on the utilization side are proteins involved in mitochondrial/cytoplasmic ADP-ATP exchange, phosphate transfer, and fuel sensing and ATPases involved in  $Ca^{2+}$  uptake and actomyosin crossbridging. While several transcription factors are known to play essential roles in heart development and the control of energy metabolism (Huss and Kelly, 2004; Olson, 2006; Scarpulla, 2006), no single factor or set of related factors have been shown to integrate the regulation of energy generation and utilization in a comprehensive manner.

The estrogen-related receptors (ERRs) were the first orphan members of the superfamily of nuclear receptors to be identified, and the subfamily is now known to contain three related isoforms,  $ERR\alpha$  (NR3B1, *Esrra*),  $\beta$  (NR3B2, *Esrrb*), and  $\gamma$  (NR3B3, *Esrrg*) (Giguère, 1999; Giguère et al., 1988). Despite their structural homology with the estrogen receptors, the ERRs are not activated by estrogens or known to be activated by other natural compounds. Instead, the transcriptional activity of the ERRs is dependent on interactions with coactivators, in particular PGC-1 $\alpha$  and PGC-1 $\beta$  (Huss et al., 2002; Kamei et al., 2003; Laganière et al., 2004; Mootha et al., 2004; Schreiber et al., 2003). The functional relationship between the ERRs and PGC-1 coactivators is of significant interest as these coactivators are known to play essential roles in mitochondrial biogenesis (reviewed in Lin et al., 2005).  $ERR\alpha$  and PGC-1 $\alpha$  are coexpressed in tissues with high energy demands and are coinduced in a tissue-specific fashion developmentally and in response to physiological stresses such as fasting, exposure to cold, and physical exercise (Cartoni et al., 2005; Ichida et al., 2002; Puigserver et al., 1998; Schreiber et al., 2003;

Sladek et al., 1997). ERR $\gamma$  and PGC-1 $\beta$  are also highly expressed in mitochondria-rich tissues with high energy needs such as the heart, kidneys, and brown adipose tissue (Hong et al., 1999; Lin et al., 2002). In addition, overexpression of PGC-1 $\alpha$  leads to a global increase in mitochondrial number and function and has been shown to selectively drive a FAO program involving ERR $\alpha$  in cardiac and skeletal myocytes (Huss et al., 2004; Mootha et al., 2004; Schreiber et al., 2004; Wende et al., 2005). It was observed that the promoters of PGC-1 $\alpha$ -induced genes often contain nuclear receptor core half-sites that resemble putative ERR and other orphan nuclear receptor binding sites (Mootha et al., 2004) and that inhibiting ERR $\alpha$  activity by using a siRNA or a small inverse agonist in cultured cells reduces the ability of PGC-1 $\alpha$  to induce respiration and mitochondrial biogenesis (Mootha et al., 2004; Schreiber et al., 2004). Taken together, these studies provide a strong basis for further investigating the functional roles of ERR $\alpha$  and evaluating the function of other ERR isoforms in energy metabolism.

Location analysis of transcription factor occupancy by a combination of chromatin immunoprecipitation (ChIP) and genomic DNA arrays (ChIP-on-chip) is a powerful tool that allows the unbiased identification of direct targets bound by a given factor or sets of factors (reviewed in Blais and Dynlacht, 2005). In particular, analysis of binding sites for nuclear receptors has revealed biological pathways controlled by a given receptor in a specific tissue or under a particular physiological condition, as well as new features of transcriptional control (Carroll et al., 2005, 2006; Cheng et al., 2006; Laganière et al., 2005; Odom et al., 2004). In this study, we have used a combination of ChIP-on-chip and expression profiling approaches to identify the promoters to which ERR $\alpha$  and  $\gamma$  bind in the adult mouse heart and to investigate changes in gene and protein expression when levels of ERR $\alpha$  are manipulated in vivo and ex vivo. Our results demonstrate that ERR $\alpha$  and  $\gamma$  act as global and physiologically relevant pleiotropic regulators of heart functions.

## RESULTS

### ChIP-on-Chip Analysis of ERR $\alpha$ and $\gamma$ Binding

In order to identify genes directly regulated by ERR $\alpha$  and  $\gamma$  in the heart of adult mice in a genome-wide manner, we used ChIP with antisera developed against ERR $\alpha$  and  $\gamma$  and a custom DNA microarray containing the region spanning 800 bp upstream and 200 bp downstream of transcriptional start sites of 18,657 mouse genes. We identified 195 and 231 ( $p \leq 0.01$ ) promoters bound by ERR $\alpha$  and  $\gamma$ , respectively, and a significant overlap between the targets of the two ERR isoforms was observed (Figure 1A, top panel; see also Figure S1 and Table S1 in the Supplemental Data available with this article online). We used Gene Ontology (GO) (Al-Shahrour et al., 2004) annotations and NCBI gene descriptions to classify the ERR $\alpha$  and  $\gamma$  target genes into functional categories and found that, collectively, the two receptors regulate a wide array of cellular processes and molecular functions

(Figure 1B and Table S1). Consistent with the proposed role of ERR $\alpha$  in the regulation of mitochondrial functions, a significant number of target genes encode proteins involved in OXPHOS and the TCA cycle. Indeed, three previously validated ERR $\alpha$  targets, *Acadm*, *Cyca*, and *Atp5b*, are included in this group (Mootha et al., 2004; Schreiber et al., 2004; Sladek et al., 1997; Vega and Kelly, 1997). However, validation of our ChIP-on-chip data as described below considerably expands the repertoire of direct mitochondrial ERR targets. Among the identified mitochondrial targets were components of the TCA cycle (*Fh1*, *Sdha*, *Sdhb*, and *Sdhc*), electron-transferring flavoproteins (*Etfb* and *Etfhd*), numerous constituents of the OXPHOS machinery (e.g., *Atp5g3*, *Coq7*, *Cox6c*, and *Ndufa8*), and genes involved in energy transfer (*Ckmt2* and *Slc25a4*, better known as ANT1) and amino acid metabolism (*Got2*). The two ERRs were also found to bind to the *Cyp27a1* promoter. CYP27A1 is a mitochondrial-membrane-bound member of the cytochrome P450 superfamily of enzymes that play an important role in cholesterol metabolism.

Other target genes directly link the ERRs with the regulation of glucose and FA metabolism. These genes include the previously validated ERR $\alpha$  target *Pdk4* (Araki and Motojima, 2006; Wende et al., 2005) and also *Slc2a12* (Glut12), *Hk2* (hexokinase 2), *H6pd* (glucose-6-phosphate dehydrogenase), *Ldhd* (lactate dehydrogenase B), *Vldlr* (very low-density lipoprotein receptor), *Slc25a29* (CACL, palmitoylcarnitine transporter), and *Fabp3* (H-FABP). Although not found by ChIP-on-chip due to the design of the array, both ERR $\alpha$  and  $\gamma$  were found to bind to the first intron of *Glut4* by standard ChIP (data not shown). Also included among the ERR targets were genes specifically involved in muscle function such as *Casq2* (calsequestrin 2), *Ldb3* (cypher), and *Tcap* (telethonin). The ERRs also bind to the promoter regions of several genes encoding transcription factors such as the well-characterized targets *Esrra* (ERR $\alpha$ ) and *Gabpa* (NRF-2) (Laganière et al., 2004; Mootha et al., 2004) and also *Rara* (RAR $\alpha$ ) and *Trp53* (p53). The two ERRs also control genes encoding coregulatory proteins such as *Mycbp* (AMY-1); *Trrap*, a pCAF-associated factor and regulator of both c-Myc and p53; *Snw1*, which encodes SKIIP, a coregulator of RAR $\alpha$  and the vitamin D receptor; and *Pias3*, an inhibitor of STAT3.

### ERR $\alpha$ and $\gamma$ Target the Same Promoters and Function as Heterodimers In Vivo

Independent location analyses with antisera to ERR $\alpha$  and  $\gamma$  showed a significant overlap between ERR $\alpha$  and  $\gamma$  target promoters set at the high-confidence arbitrary threshold of  $p \leq 0.01$  (Figure 1A, top panel and Table S1). Validation of a large number of target promoters obtained at this threshold by standard PCR ChIP showed that ERR $\alpha$  and  $\gamma$  were indeed binding to all of their respective promoters identified by ChIP-on-chip, indicating that by arbitrarily defining the threshold at  $p \leq 0.01$ , several targets were missed for both receptors (Figure 1C and Figure S2). Despite a similar overlap between ERR $\alpha$  and  $\gamma$  target

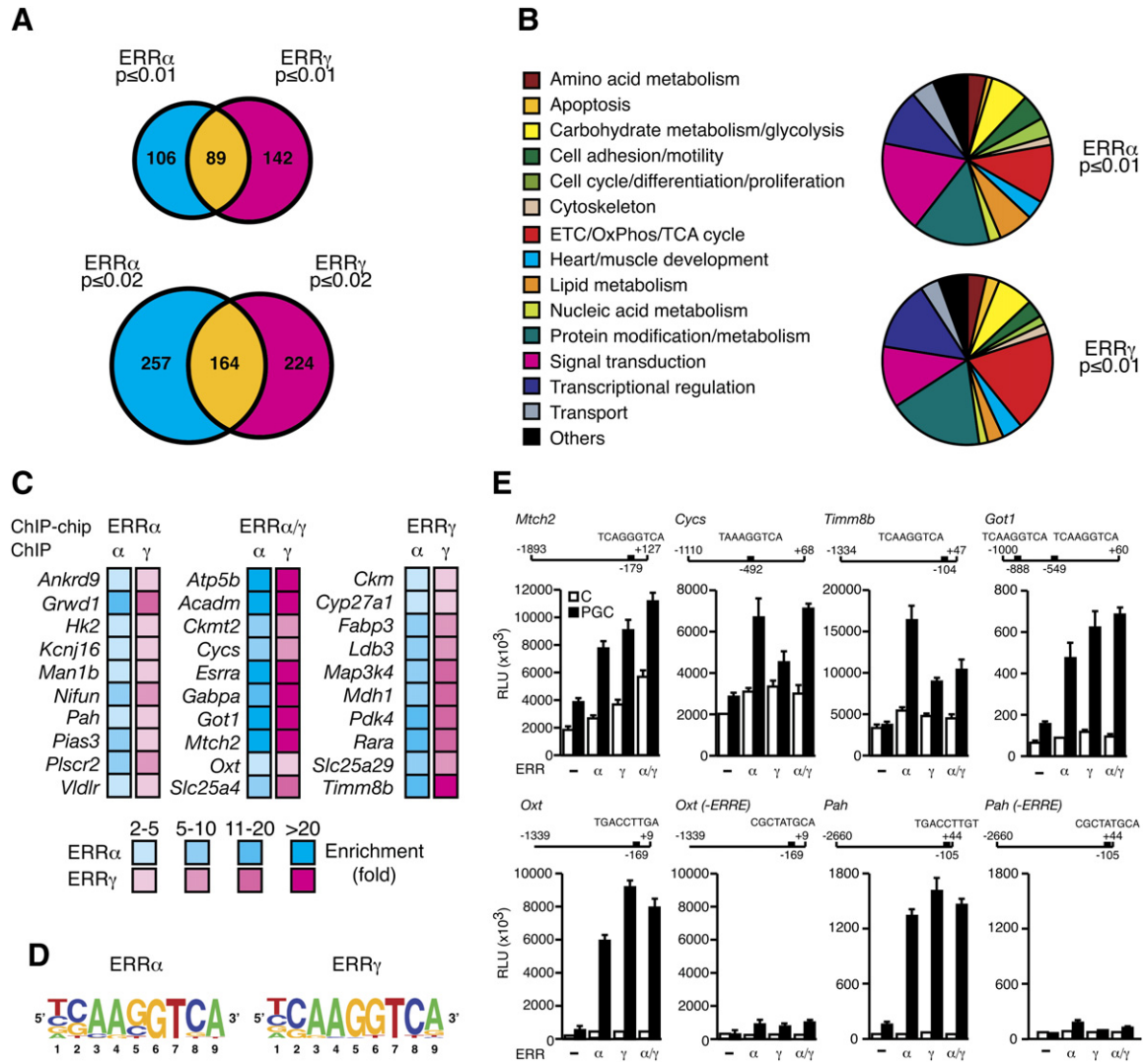


**Figure 1. Genome-wide Promoter Occupancy of ERR $\alpha$  and  $\gamma$  in Cardiac Tissue**

(A) Venn diagrams illustrating the overlap in ERR $\alpha$  and  $\gamma$  direct targets obtained from ChIP-on-chip analyses in mouse heart at p  $\leq$  0.01 (top panel) and p  $\leq$  0.02 (bottom panel).

(B) Pie charts representing the major cellular functions associated with ERR $\alpha$  and  $\gamma$  targets enriched in the adult mouse heart at a cutoff of p  $\leq$  0.01.

(C) Standard ChIP validation of ERR $\alpha$  and  $\gamma$  ChIP-on-chip target genes in mouse heart at a cutoff of p  $\leq$  0.01. Promoters found to be bound by either ERR $\alpha$  or  $\gamma$  or by both nuclear receptors in the ChIP-on-chip experiments were all found to be occupied ( $\geq$ 2-fold enrichment) by both receptors when tested by standard ChIP assays. The results shown are from one experiment based on three independent immunoprecipitations prepared from a pool of 20 hearts.

(D) Motif-finding algorithms revealed that the consensus ERR response element (ERRE) was found in 69% and 74% of the ERR $\alpha$  and  $\gamma$  target promoters used in the analysis, respectively.

(E) Activation of target promoters by ERR $\alpha$  and  $\gamma$ . Each panel displays a schematic representation of the target promoter sequences cloned upstream of the luciferase reporter gene and the results of cotransfection assays in COS-1 cells with empty vector, ERR $\alpha$ , ERR $\gamma$ , or combined ERR $\alpha$  and  $\gamma$  expression vectors in the presence (PGC, black bars) or absence (C, white bars) of PGC-1 $\alpha$ . To test for ERRE-dependent activation of the *Oxt* and *Pah* promoters by ERR $\alpha$  and  $\gamma$ , the identified ERREs were replaced with the CGCTATGCA sequence. Data are shown in relative luciferase units (RLUs) and are presented as mean  $\pm$  SEM.

promoters when comparison was made using data sets obtained with p  $\leq$  0.02 (Figure 1A, bottom panel), many of the missed ERR targets at p  $\leq$  0.01 were found using this less stringent cutoff. These results suggested that ERR $\alpha$  and  $\gamma$  may in fact bind the same repertoire of promoters in the adult heart. We tested this consideration by performing standard PCR ChIP assays with ERR $\alpha$

and  $\gamma$  antisera on individual promoters originally identified by ChIP-on-chip using the ERR $\gamma$  and  $\alpha$  antisera, respectively (Figure 1C and Figure S2). For example, while *Hk2*, *Plscr2*, and *Vldlr* were identified as ERR $\alpha$  targets in the ChIP-on-chip experiment, standard ChIP assays showed these promoters to be equally enriched by the ERR $\gamma$  antiserum. Conversely, the *Fabp3*, *Ldb3*, and *Timm8b/Sdh*

promoters were originally identified as ERR $\gamma$  targets, but standard ChIP assays also demonstrated their regulatory regions to be targets for ERR $\alpha$ .

The results of the genome location analysis were further validated by using a motif-finding algorithm that inspects the ChIP-on-chip selected sequences and searches for DNA sequence motifs representing the protein:DNA interaction sites (Liu et al., 2002). The consensus sequences derived from the most frequent motifs found in the ERR $\alpha$ - or  $\gamma$ -bound promoters both correspond to the ERR response element (ERRE; TCAAGGTCA, Figure 1D) (Sladek et al., 1997), indicating that both receptor isoforms recognize the same target sequence. We next examined whether target promoters identified by ChIP-on-chip experiments were indeed responsive to ERR $\alpha$  and  $\gamma$ . We tested six promoters containing one or more consensus ERREs, including the previously validated ERR $\alpha$  target *Cyca*, by measuring their response in a cotransfection assay to ERR $\alpha$ , ERR $\gamma$ , or a combination of both receptors in the presence or absence of the coactivator PGC-1 $\alpha$  (Figure 1E). While promoters displayed individual variations in the potency of the response to the receptors (from 1.5- to 50-fold), all promoters responded to the presence of ERR $\alpha$  and  $\gamma$ . The basal transcriptional activity of both ERR isoforms is generally low in the absence of external stimuli but in most instances can be forcefully increased by the introduction of PGC-1 $\alpha$ . As expected, ERR $\alpha$  and  $\gamma$  were found to directly bind to the indicated ERREs (Figure 1E and Figure S3), while mutations of the ERREs in the *Oxt* and *Pah* promoters significantly reduced the transcriptional activity of ERR $\alpha$  and  $\gamma$  on these promoters (Figure 1E, lower panels).

ERR $\alpha$  is known to bind to the ERRE as both a dimer and a monomer (Barry et al., 2006; Laganière et al., 2004). Analysis and validation of the ChIP-on-chip experiments showed that ERR $\alpha$  and  $\gamma$  share the same target promoters and recognize the same ERRE binding motif. Thus, one possible interpretation of these data is that the two ERR isoforms could form functional heterodimers. We first tested whether ERR $\alpha$  and  $\gamma$  could bind an ERRE as heterodimers in vitro. As shown in Figure 2A (left panel), coexpression of the two receptor isoforms leads to the formation of an intermediate band in the gel shift assay, indicating the presence of an ERR $\alpha$ / $\gamma$  heterodimer in the binding reaction. Furthermore, all three ERR complexes (ERR $\alpha$ / $\alpha$ , ERR $\alpha$ / $\gamma$ , and ERR $\gamma$ / $\gamma$ ) could be supershifted in the presence of a PGC-1 $\alpha$  fragment containing the LxxLL interaction motifs, demonstrating that both homodimer and heterodimer complexes recognize their coactivator "ligand" (Figure 2A, right panel).

We next determined whether ERR $\alpha$  and  $\gamma$  interact in vivo. We first subjected lysates prepared from wild-type hearts to immunoprecipitation with anti-ERR $\alpha$  or anti-ERR $\gamma$  antisera followed by western blotting with anti-ERR $\alpha$  or anti-ERR $\gamma$  antisera. As shown in Figure 2B, ERR $\alpha$  could be detected in the extract immunoprecipitated with the ERR $\gamma$  antiserum (top panel), while ERR $\gamma$  could be detected in the extract immunoprecipitated with the ERR $\alpha$  antiserum (bottom panel). As a control, we

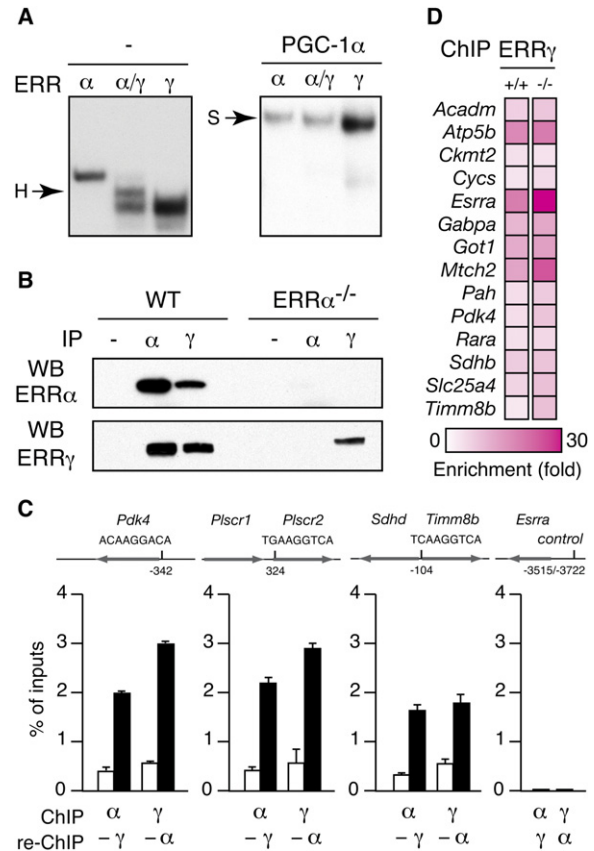


**Figure 2. ERR $\alpha$  and  $\gamma$  Form Heterodimers, but ERR $\alpha$  Is Not Essential for ERR $\gamma$  Promoter Occupancy in the Mouse Heart**  
 (A) ERR $\alpha$  and  $\gamma$  form functional heterodimers in vitro. ERR $\alpha$ ,  $\Delta$ N-ERR $\gamma$ , or both proteins together were incubated with an ERRE probe with (right panel) or without (left panel) a GST-PGC-1 $\alpha$  fusion protein. H and S indicate the heterodimeric ERR $\alpha$ / $\gamma$  complex and the supershifted ERR/PGC-1 $\alpha$  complexes, respectively.  
 (B) ERR $\alpha$  and  $\gamma$  interact in vivo. Lysates from wild-type (WT) and ERR $\alpha$  null hearts were subjected to immunoprecipitation with either anti-ERR $\alpha$  or anti-ERR $\gamma$  antibodies and then subjected to immunoblot analysis with either anti-ERR $\alpha$  (top lane) or anti-ERR $\gamma$  (bottom lane).  
 (C) Re-ChIP experiments performed on the *Pdk4*, *Plscr2*, and *Timm8b*/*Sdhb* promoters as well as on a control region using either anti-ERR $\alpha$  or anti-ERR $\gamma$  antibodies in a serial manner. The results shown are from one experiment based on two independent immunoprecipitations prepared from a pool of 20 hearts; error bars represent standard deviation.  
 (D) ERR $\gamma$  promoter occupancy in ERR $\alpha$  null hearts. ERR $\gamma$  was found to be enriched at ERR target promoters identified by ChIP-on-chip experiments despite the absence of ERR $\alpha$  as determined by standard ChIP assays. The results shown are from one experiment based on three independent immunoprecipitations prepared from a pool of 20 hearts.

performed the same experiment using lysates prepared from hearts obtained from ERR $\alpha$  null mice. As expected, only ERR $\gamma$  could be detected, and only when the proteins were immunoprecipitated using the ERR $\gamma$  antiserum. To further demonstrate that ERR $\alpha$  and  $\gamma$  form heterodimeric complexes on chromatin, we performed serial ChIP experiments. The *Pdk4*, *Plscr2*, and *Timm8b*/*Sdhb* promoters, but not the control region, were enriched after serial ChIP

**Table 1. Enrichment p Values of Top Ranking Factors Predicted in ERR $\alpha$ / $\gamma$  Target Promoters**

Module	Factor	All	ERRE+	ERRE-
M00511	ERR $\alpha$	$3 \times 10^{-18}$	NA	NA
M00225	STAT3	$6 \times 10^{-3}$	$3 \times 10^{-4}$	0.54
M00652	NRF-1	$6 \times 10^{-2}$	$6 \times 10^{-5}$	0.88
M00224	STAT1	$6 \times 10^{-3}$	$1 \times 10^{-4}$	0.67
M00039	CREB	$2 \times 10^{-6}$	$6 \times 10^{-4}$	$9 \times 10^{-3}$

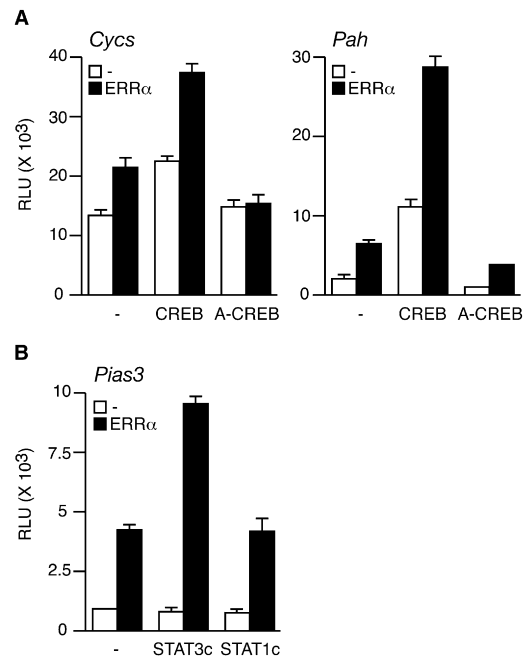
p values in italics indicate significant enrichment of associated transcription factor binding sites. NA = not applicable.

(Figure 2C), demonstrating that ERR $\alpha$  and  $\gamma$  are recruited together at the same genomic locations. It is important to note that the primers specific for the target promoters amplify genomic regions containing a single identified ERRE (Figure 2C). We next tested whether the presence of ERR $\alpha$  was required for ERR $\gamma$  to recognize ERR target genes. We thus performed standard ChIP assays using the ERR $\gamma$  antiserum and chromatin isolated from wild-type and ERR $\alpha$  null hearts on 14 different target promoters (Figure 2D). The levels of enrichment of ERR $\gamma$  at these promoters were either comparable or slightly higher when tested with chromatin isolated from ERR $\alpha$  null hearts, indicating that ERR $\gamma$  can bind DNA efficiently in the absence of ERR $\alpha$ .

### CREB and STAT3 Partner with the ERRs to Activate Metabolic Target Genes

To identify cooperating factors that could modulate ERR $\alpha$  and  $\gamma$  function, we first searched ERR target promoters for known transcription factor binding sites. The set of TRANSFAC position-weight matrices whose sites are enriched within the ERR target promoters obtained from our ChIP-on-chip assays are shown in Table 1. In agreement with the results obtained with the motif-finding algorithm (Figure 1D), the hits for ERR (matrix M00511) are the most enriched. Analyzing the ERRE-containing regions and the non-ERRE-containing regions separately, we found that STAT1 (matrix M00224), STAT3 (matrix M00225), and NRF-1 (matrix M00652) are highly enriched in the ERRE-containing promoters, but not in the non-ERRE-containing regions. On the other hand, binding sites for CREB appear to be enriched in both ERRE- and non-ERRE-containing promoters.

We next examined whether the presence of CREB and STAT binding sites has functional significance for ERR $\alpha$  function. The *Cyca* promoter is a validated ERR $\alpha$  target that also contains a CREB binding site (Schreiber et al., 2004; Zhang et al., 2005). The *Cyca* promoter was thus fused to the luciferase reporter gene, and the construct was cotransfected together with expression vectors for ERR $\alpha$  and CREB in the presence of the ERR $\alpha$  coactivator "ligand" PGC-1 $\alpha$ . As shown in Figure 3A, ERR $\alpha$  and CREB display small but significant transcriptional activities on the *Cyca* promoter. However, when added together, a much more potent activation of the *Cyca* promoter

**Figure 3. Functional Interaction between ERR $\alpha$ , CREB, and STAT3 on ERR Target Promoters**

(A) CREB is required for the PGC-1 $\alpha$ -induced transcriptional activity of ERR $\alpha$  on the *Cyca* and *Pah* promoters. Dominant-negative CREB (A-CREB) abrogated the activation observed with ERR $\alpha$ . Data in (A) and (B) are shown in relative luciferase units (RLUs) and are presented as mean  $\pm$  SEM.

(B) STAT3 specifically synergizes the activity of ERR $\alpha$  on the *Pias3* regulatory region. A *Pias3* luciferase reporter construct was cotransfected with empty vector or an ERR $\alpha$  expression vector in the presence of constitutively active STAT3 (STAT3c) or STAT1 (STAT1c).

was observed. Interestingly, introduction of a dominant-negative form of CREB (A-CREB) abolished the transcriptional activity of ERR $\alpha$  on the *Cyca* promoter, indicating that the action of CREB is required for ERR $\alpha$  function on this particular promoter. Similar results were obtained when using a *Pah* reporter construct also containing a CREB binding site (Figure 3A). As a control, we used the *Pias3* regulatory region lacking a CREB binding motif to ensure that the effect seen by CREB and A-CREB on ERR $\alpha$  activity on the *Cyca* and *Pah* promoters is dependent on the presence of a functional CREB binding site (Figure S4). As predicted, CREB and A-CREB had no effect on the ERR $\alpha$  transcriptional response with the *Pias3* regulatory region. We next investigated the action of ERR $\alpha$  with STAT1 or STAT3 on the *Pias3* regulatory region. *Pias3* is an interesting ERR target, as this factor, a known inhibitor of STAT3 function, could be involved in a regulatory feedback loop. Figure 3B shows that ERR $\alpha$  is a potent activator of *Pias3*. On the other hand, constitutively active forms of both STAT1 (STAT1c) and STAT3 (STAT3c) failed to activate transcription from the *Pias3* regulatory region. However, cotransfection of ERR $\alpha$  and STAT3c resulted in a synergistic action of the two factors, while STAT1c had no effect.

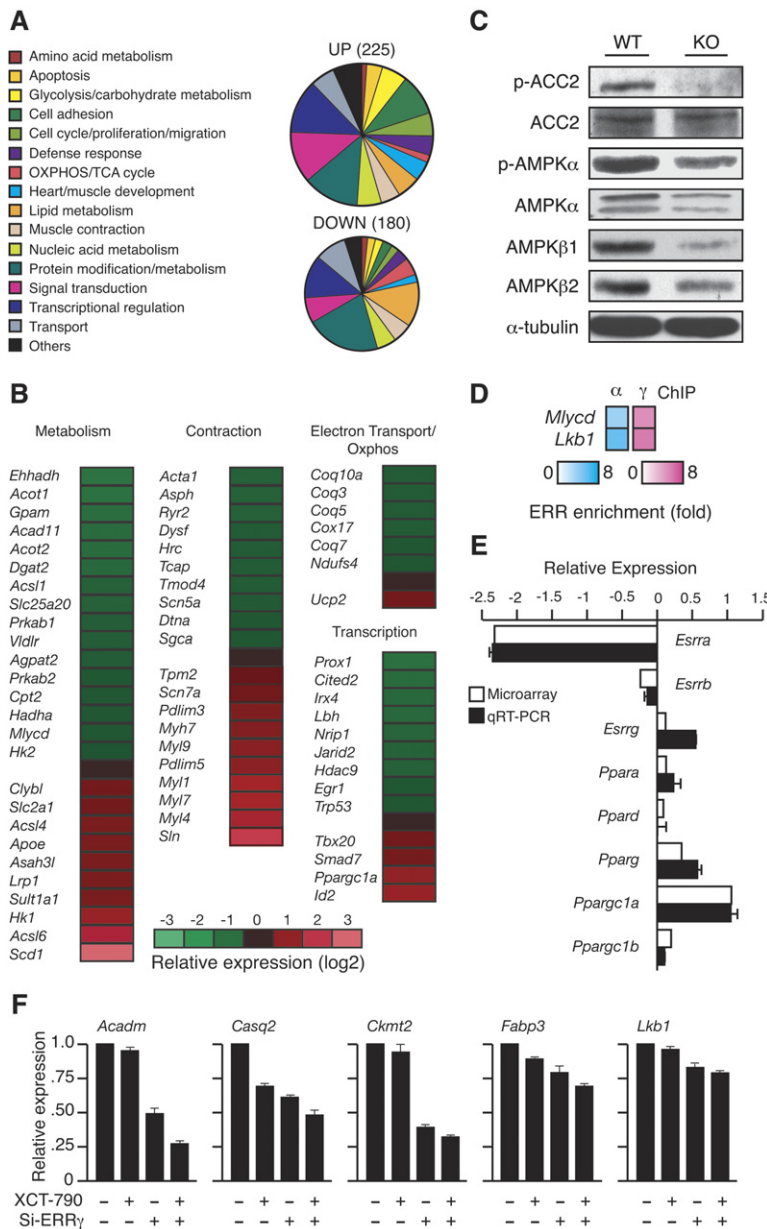


**Figure 4. Gene Expression Profiling in ERR $\alpha$  Null Hearts**

(A) Pie charts representing the major cellular functions of upregulated and downregulated genes in mouse hearts lacking ERR $\alpha$  at a cutoff of  $p \leq 0.001$  and relative fold change  $(\log_2) \pm 0.5$ .

(B) Schematic representation of a set of differentially regulated genes involved in selected biological processes expressed as relative fold change  $(\log_2)$ .

(C) Hearts lacking ERR $\alpha$  have more active acetyl-CoA carboxylase  $\beta$ . Protein lysates from wild-type and ERR $\alpha$  null mouse hearts were probed with antibodies against phospho-ACC, ACC, phospho-AMPK $\alpha$ , AMPK $\alpha$ , and AMPK $\beta$ 1 and 2. Immunoblotting with anti- $\alpha$ -tubulin served as a control for equal loading.

(D) Standard ChIP validation of ERR $\alpha$  and  $\gamma$  binding to targets not identified in the original ChIP-on-chip experiment that are involved in the fuel-sensing pathway. The results shown are from one experiment based on three independent immunoprecipitations prepared from a pool of 20 hearts.

(E) Real-time qRT-PCR performed on RNA isolated from adult mouse hearts used in the microarray analysis. Relative fold  $(\log_2)$  expression levels were normalized to  $\beta$ -actin levels and are presented as mean  $\pm$  SEM.

(F) Additive effect of the loss of ERR $\alpha$  and  $\gamma$  regulation on target gene expression. Relative expression of ERR $\alpha$  and  $\gamma$  target genes not significantly altered in ERR $\alpha$  null hearts is affected by the simultaneous loss of ERR $\gamma$  expression and inhibition of ERR $\alpha$  activity. Quantitative real-time PCR was performed on RNA isolated from mouse HL-1 atrial myocytes stably expressing either GFP or a siERR $\gamma$ -encoding adenovirus following treatment with vehicle (0.1% DMSO) or the ERR $\alpha$  inverse agonist XCT790 (1  $\mu$ M) for 24 hr. Results of two independent experiments performed in duplicate are shown as the mean  $\pm$  SEM of relative fold expression levels normalized to *Arbp* levels.

### Expression Profiling and Disruption of the Fuel-Sensing Pathway in ERR $\alpha$ Null Mice

To further explore the role of ERR $\alpha$  in the heart, we next examined the effects of loss of ERR $\alpha$  function on global gene expression in the heart. The results first revealed that more genes are upregulated than downregulated (225 versus 180) in the ERR $\alpha$  null heart (Figure 4A). GO analysis of the microarray data set shows that genes involved in heart and muscle development, muscle contraction, lipid metabolism, OXPHOS, protein metabolism, and transcription are well represented (Figure 4A). Changes in the expression of transcription factors and coregulators having important roles in myocardial development and function such as *Irx4*, *Egr1*, *Jarid2*, and *Id2* are shown (Figure 4B). Interestingly, ERR $\alpha$  and  $\gamma$  bind to a regulatory

region located  $\sim 4.7$  kb upstream of the *Jarid2* transcription start site (TSS), suggesting that *Jarid2* is also a direct ERR target (data not shown). In addition, the expression levels of several genes encoding proteins involved in Ca<sup>2+</sup> handling and muscle contraction (e.g., *Acta1*, *Hrc*, *Ryr2*, *Tcap*, *Myl1*, *Myl4*, *Myl7*, *Myl9*, *Pdlim3*, *Pdlim5*, and *Sln*) were altered. Moreover, genes involved in glucose (*Glut1* and *Hk2*) and FA (*Vldlr*, *Cpt2*, and *Hadha*) metabolism were found to be deregulated in ERR $\alpha$  null hearts. As expected, several OXPHOS genes (e.g., *Coq7* and *Ndufs4*) were downregulated. On the other hand, changes in the expression levels of the AMPK $\beta$  subunits (*Prkab1* and *Prkab2*) as well as malonyl-CoA decarboxylase (*Mlycd*) revealed an important role for ERR $\alpha$  in fuel sensing.

The downregulation of *Prkab1* and *Prkab2* expression coincided with a decrease in AMPK $\beta$ 1 and AMPK $\beta$ 2 protein levels (Figure 4C). Although the expression levels of the AMPK $\alpha$  subunits were not significantly altered in the ERR $\alpha$  null hearts validated by qRT-PCR validation (data not shown), the AMPK $\alpha$ 1 and AMPK $\alpha$ 2 protein levels were found to be decreased in the ERR $\alpha$  null mice (Figure 4C). In addition, we also examined whether AMPK activity would be affected in the ERR $\alpha$  null heart. As can be observed in Figure 4C, phosphorylation of the catalytic  $\alpha$  subunit of AMPK at Thr172 is reduced. Accordingly, we also found decreased phosphorylation of ACC2, the prime target of AMPK in the control of FAO (reviewed in Kahn et al., 2005). ACC2 catalyzes the conversion of acetyl-CoA to malonyl-CoA, which inhibits CPT1, the rate-limiting step in FA metabolism (Abu-Elheiga et al., 2000). Mice lacking ACC2 exhibit increased rates of FAO in both the heart and skeletal muscle, where ACC2 is found to be primarily expressed (Abu-Elheiga et al., 2001). Interestingly, ERR $\alpha$  and  $\gamma$  were found to be enriched by standard ChIP at the first intron of *Cpt1a* (data not shown). Taken together, the downregulation of *Mlycd* (MCD) expression and potential increased ACC2 activity (as predicted by a reduction in phosphorylation status) in the ERR $\alpha$  null heart suggests an important role for ERR $\alpha$  in the maintenance of the cellular energy-sensing apparatus. Finally, because some promoters were absent from our genomic DNA array, we examined whether ERR $\alpha$  and  $\gamma$  could directly target additional genes that play a role in the energy-sensing apparatus. Of particular interest, we found that *Lkb1* (*Stk11*), which encodes the physiologically relevant AMPK kinase (AMPKK), and *Mlycd* regulatory regions could be enriched with both ERR $\alpha$  and  $\gamma$  antisera (Figure 4D).

Overall, 14 ERR $\alpha$  and  $\gamma$  target genes identified by ChIP-on-chip were found to be altered in the ERR $\alpha$  null hearts. The differential expression of these genes, including *Hk2*, *Vldlr*, *Coq7*, *Eno1*, *Tcap*, and *Trp53*, had no relation to whether they were found to be targets of ERR $\alpha$  or ERR $\gamma$  or were common to both at  $p \leq 0.01$ . In the cluster associated with transcription (Figure 4B), the ERR corepressor *Nrip1* (RIP-140) was downregulated while expression of the coactivator *Ppargc1a* (PGC-1 $\alpha$ ) was elevated, suggesting a mechanism to compensate for the absence of ERR $\alpha$ . This suggestion was strengthened by the observation that, in addition to higher levels of PGC-1 $\alpha$ , the relative expression of ERR $\gamma$  and PPAR $\gamma$  was also elevated in the hearts of ERR $\alpha$  null mice (Figure 4E). In agreement with these observations, ERR $\alpha$  null hearts exhibit only modest differences in the expression of critical enzymes involved in mitochondrial ATP synthesis (Figure S5). To further test this hypothesis, HL-1 cardiomyocytes stably expressing GFP or GFP and a siERR $\gamma$ -encoding adenovirus were treated with a selective ERR $\alpha$  inverse agonist, and qRT-PCR was performed on ERR $\alpha$  and  $\gamma$  target genes not significantly altered in the ERR $\alpha$  null hearts (Figure 4F). The ERR $\alpha$  inverse agonist XCT790 alone had little effect on the expression of target genes, similar to the results observed in hearts lacking ERR $\alpha$ . A more significant

reduction in transcript levels was seen in cardiomyocytes expressing a siRNA against ERR $\gamma$ , with an added decrease in expression when treated with XCT790.

We next sought to further explore the potential for ERR $\alpha$  and  $\gamma$  to regulate cardiac contractile and Ca<sup>2+</sup> handling proteins by introducing exogenous ERR $\alpha$  and  $\gamma$  in cardiac myocytes. To this end, we used adenovirus to efficiently express ERR $\alpha$  or  $\gamma$  in rat neonatal cardiac myocytes, a model used in previous studies to demonstrate activation of FA uptake and mitochondrial oxidation genes by ERR $\alpha$  (Huss et al., 2004). Analysis of structural and contractile proteins revealed that ERR $\alpha$  and  $\gamma$  robustly activated transcripts encoding contractile protein isoforms specifically expressed in adult ventricles, whereas they had differential effects on isoforms specific to skeletal myocytes or to atria (Figure 5A). In addition, immunofluorescence detection of  $\alpha$ -tubulin,  $\alpha$ -actinin, and cardiac troponin I (TnI) showed that exogenous expression of ERR $\alpha$  increased cardiac myocyte cytoskeletal and myofibril protein density and organization (Figure 5B). As predicted by microarray analyses, ERR $\alpha$  and  $\gamma$  activated two genes involved in sarcoplasmic reticulum (SR) Ca<sup>2+</sup> handling, SR Ca<sup>2+</sup>-ATPase (*Atp2a2*) and its regulatory partner phospholamban (*Pln*) (Figure 5A). Furthermore, standard ChIP analysis of the genes involved in contraction and Ca<sup>2+</sup> handling identified ERR $\alpha$  and  $\gamma$  regulatory binding sites in the proximity of the *Myh6*, *Myh7*, *Actc1*, *Atp2a2*, and *Pln* genes not identified by ChIP-on-chip studies (Figure 5C). Collectively, these results support the overlapping regulatory functions of ERR $\alpha$  and  $\gamma$  in cardiac genes engaged in energy synthesis and utilization.

## DISCUSSION

The heart is a specialized organ that must relentlessly produce enough ATP from glucose and FA oxidation to sustain intracellular Ca<sup>2+</sup> homeostasis and contraction. To maintain its essential function, the heart must regulate a cascade of biological processes including (1) the uptake and cytoplasmic processing of energy substrates; (2) the production of ATP via glucose and FA oxidation, the TCA cycle, and OXPHOS; (3) the transport of ATP across the mitochondrial membranes and generation of the phosphocreatine pool by creatine kinase; (4) the sensing of cellular energy charge through the LKB1/AMPK/ACC2/MCD pathway; and (5) Ca<sup>2+</sup> handling and contractile work. In this study, the combined use of genome-wide location and differential gene expression analyses showed that the orphan nuclear receptors ERR $\alpha$  and  $\gamma$  control all aspects of this integrated process by regulating the expression of genes involved at each step (Figure 6).

Our data show that ERR $\alpha$  and  $\gamma$  target a common set of promoters, can exist in a heterodimer form in the heart, and convey transcriptional activation by PGC-1 $\alpha$ . These results therefore support a model in which ERR isoforms act in concert to regulate a broad genetic program essential for proper heart function. It is highly likely that ERR $\beta$ , the third member of the ERR subfamily expressed in the heart (Bookout et al., 2006; Giguère et al., 1988), also

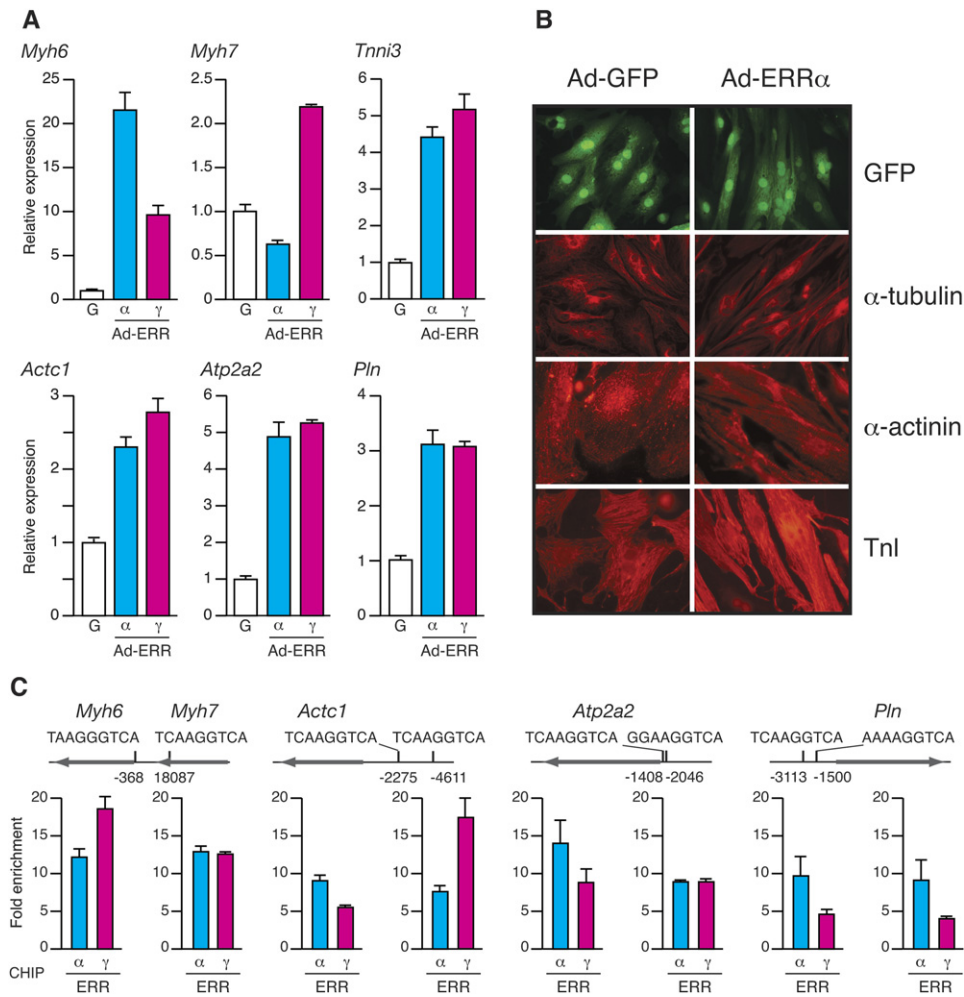


**Figure 5. ERR $\alpha$  and  $\gamma$  Regulation of Genes Encoding Contractile and Ca<sup>2+</sup> Handling Proteins Involved in Excitation-Contraction Coupling in Cardiac Myocytes**

(A) Quantitative real-time PCR was performed on RNA isolated from rat neonatal ventricular myocytes expressing GFP, ERR $\alpha$ , or ERR $\gamma$  via adenoviral infection. Primers were specific for  $\alpha$ -myosin heavy chain (*Myh6*),  $\beta$ -myosin heavy chain (*Myh7*), cardiac troponin I (*Tnni3*),  $\alpha$ -cardiac actin (*Actc1*), Ca<sup>2+</sup>-ATPase (*Atp2a2*), and phospholamban (*Pln*). Data are reported as mean  $\pm$  SEM arbitrary units internally normalized to *Arbp* expression and relative to GFP (=1.0).

(B) Fluorescence microscopy analysis of Ad-GFP- or Ad-ERR $\alpha$ -infected rat neonatal cardiac myocytes. Visualization of GFP, which is expressed from a separate expression cassette in the adenovirus construct, reveals evidence of morphology changes induced by ERR $\alpha$  expression. ERR $\alpha$  increases cardiac myocyte cytoskeletal and myofibril protein density and organization as evidenced by immunofluorescence detection of  $\alpha$ -tubulin,  $\alpha$ -actinin, and cardiac troponin I (Tnl).

(C) Standard ChIP quantitative PCR analysis of genes involved in contraction and Ca<sup>2+</sup> handling. ERR $\alpha$  and  $\gamma$  were found to be occupied at regulatory regions within the *Myh6*, *Myh7*, *Actc1*, *Atp2a2*, and *Pln* genes in mouse hearts. The results shown are from one experiment based on three independent immunoprecipitations prepared from a pool of 20 hearts; error bars represent standard deviation.

participates in this gene regulatory network. It is also probable that the distinct homodimeric and heterodimeric ERR complexes, whose relative abundance is dictated by their levels of expression in a particular tissue, may display differential and cell-specific transcriptional activity. However, the observation that the ERR $\alpha$  null mouse is viable and fertile and displays no vital physiological abnormalities in the resting state (Luo et al., 2003) provides further evidence that the other two ERR isoforms can compensate for its absence under favorable physiological conditions. Indeed, the presence of ERR $\alpha$  is not absolutely

required for ERR $\gamma$  binding to ERR target promoters (Figure 2D). Of particular interest, in the ERR $\alpha$  null heart, the corepressor *Nrip1* (RIP-140) is downregulated while *Ppargc1a* (PGC-1 $\alpha$ ) is upregulated at a time when the expression of *Esrg* (ERR $\gamma$ ) is also elevated, suggesting the establishment of a compensatory transcriptional control mechanism in the absence of ERR $\alpha$ . The compensatory mechanism is particularly evident in the HL-1 cardiomyocytes, where ERR $\gamma$  was shown to play an important role in maintaining the expression of ERR $\alpha$  target genes. Genetic redundancy has been documented for other members of



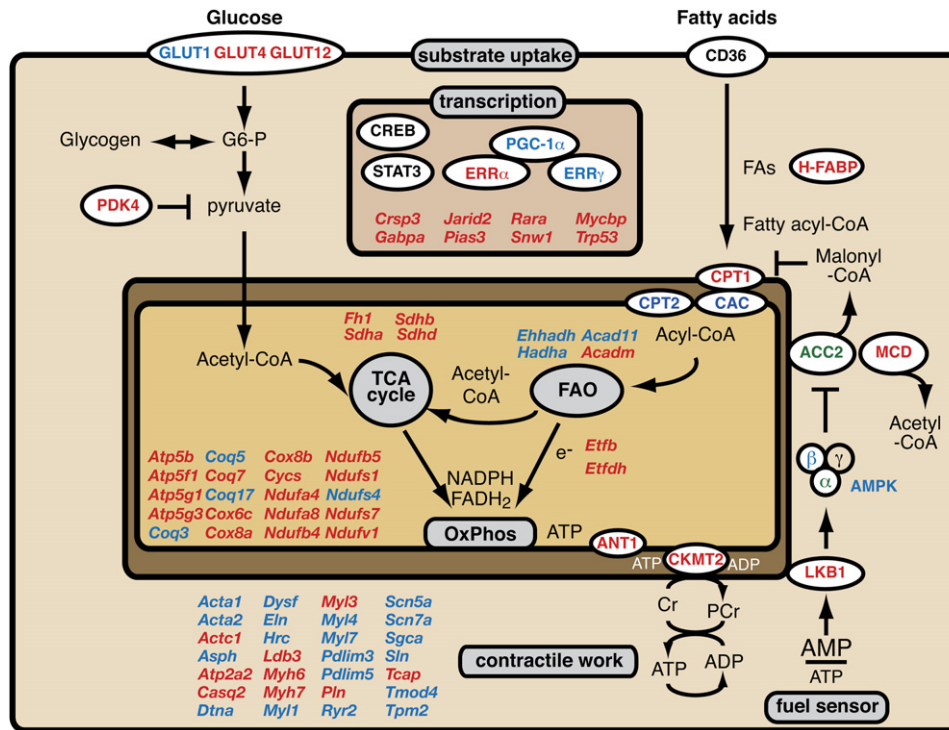


**Figure 6. Comprehensive Orchestration of Cardiac Functions by ERR $\alpha$  and  $\gamma$**

Schematic representation of biological pathways regulated by ERR $\alpha$  and  $\gamma$  in the adult mouse heart. Substrate uptake, transcription, energy production (TCA cycle, FAO, and OXPHOS), contractile work, and fuel sensing are represented as gray boxes. A partial list of ERR $\alpha$  and  $\gamma$  direct target genes are shown in red, while genes and proteins with altered levels in expression or activity in hearts lacking ERR $\alpha$  are labeled in blue and green, respectively. Important components of pathways shown for clarity but not regulated by the ERRs in this study are displayed in black. Genes identified by their official symbols are shown in italics; genes and proteins identified by their common names are shown in uppercase letters.

the nuclear receptor superfamily, most notably for the three RAR isoforms (Mark et al., 2006). However, this study demonstrates that closely related nuclear receptors target the same gene networks on a genome-wide scale and can regulate common biological processes in a tissue where they are coexpressed.

Our results not only validate the role of ERR $\alpha$  in FAO and OXPHOS but also implicate ERR $\gamma$  in this process and considerably expand the repertoire of ERR target genes and associated functions in cardiac energetics. We show that the global control of heart function by ERR $\alpha$  and  $\gamma$  also involves the direct regulation of transcriptional regulators (e.g., *Esrra*, *Gabpa*, *Rara*, *Trp53*, *Crsp3*, *Mycbp*, *Pias3*, and *Snw1*). The identification of a large number of ERR target promoters provided the opportunity to investigate whether the ERRs cooperate with other transcription factors in the heart to regulate gene networks controlling energy metabolism. In particular, we found that STAT3, STAT1, and NRF-1 binding motifs were significantly enriched in promoters containing a consensus ERRE. On the other hand, the CREB binding motif was enriched in both ERRE-containing and non-ERRE-containing regions.

NRF-1 is a factor that plays an important role in mitochondrial biogenesis and energy production (Scarpulla, 2006). It has been suggested that NRF-1 acts downstream of the initial PGC-1 $\alpha$ -induced expression of ERR $\alpha$  in

mouse myoblasts in culture (Mootha et al., 2004). Our data argue that NRF-1, as a late mediator of the mitochondrial transcriptional program induced by PGC-1 $\alpha$ , targets a set of promoters first bound by the ERRs to ensure a lasting response to the initiating physiological stimulus.

Significantly, cotransfection of STAT3 or CREB with ERR $\alpha$  showed a cooperative activation of target promoters. In addition, a dominant-negative form of CREB decreased the transcriptional activity of ERR $\alpha$  on the *Cycs* and *Pah* promoters, indicating that the action of CREB was required for ERR $\alpha$  function on these promoters. Interestingly, 53 of the ERR target promoters identified in this study were recently reported to be enriched using a CREB antibody and chromatin obtained from human HEK293T cells (Zhang et al., 2005). In addition, STAT3 has been shown to be involved in several mechanisms required for the protection of the heart from injury and failure (Hilfiker-Kleiner et al., 2005), suggesting that the functional interaction between ERR $\alpha$  and STAT3 in the heart is physiologically relevant. The identification of *Pias3* as a direct ERR target further strengthens the functional link between the ERRs and STAT3 by suggesting the existence of a feedback regulatory loop controlling the activity of the two factors.

We have demonstrated that the ERRs regulate a broad genetic program involved in every aspect of heart

function. The biological significance of the ERR target genes identified in this study is further exemplified by the knowledge that a large number of these genes have been linked to specific cardiac phenotypes in mouse models and/or cardiomyopathies in humans (Table S2). Our results suggest that ERR agonists could provide a therapeutic approach to managing diverse cardiomyopathies and preventing heart failure. Although the development of ERR $\alpha$  agonists has yet to be achieved, our data show that targeting ERR $\gamma$  could be a rational alternative (Chao et al., 2006). Finally, if the global role of ERR $\alpha$  and  $\gamma$  in the control of energy metabolism in the heart is conserved in skeletal muscle, the use of selective ERR modulators could also be envisaged as a pharmacological strategy against obesity and the metabolic syndrome.

## EXPERIMENTAL PROCEDURES

### Animals

Two- to three-month-old male wild-type and ERR $\alpha$ <sup>-/-</sup> mice (Luo et al., 2003) in a C57BL/6J genetic background were housed in the animal facility at the McGill University Health Centre and fed standard chow.

### ChIP, ChIP-on-Chip, and Quantitative Real-Time PCR

ERR $\alpha$  and  $\gamma$  ChIP assays on wild-type and ERR $\alpha$  null adult mouse hearts for standard ChIP or ChIP-on-chip studies were performed as described in Supplemental Experimental Procedures using an anti-hERR $\alpha$  polyclonal antibody raised in our laboratory against the N terminus (first 74 amino acids) or with a purified specific anti-hERR $\gamma$  polyclonal antibody raised against the ligand-binding domain (amino acids 229–458). For ChIP assays, material corresponding to 0.15 g of initial tissue weight obtained from a pool of at least 20 hearts was used for each immunoprecipitation. For triplicate genome-wide location analyses, material corresponding to 1.5 g of initial heart mass taken from 44 pooled formaldehyde-crosslinked sonicated hearts was used for each immunoprecipitation. To assess the enrichment of ERR $\alpha$  or  $\gamma$  at specific promoters, qPCR was performed using mouse heart standard ChIP samples on a Roche LightCycler instrument with a program consisting of 15 min at 95°C followed by 45 cycles of 15 s at 95°C, 30 s at 60°C, and 30 s at 72°C with a transition temperature of 20°C/s. ERR promoter occupancy was quantified using the formula

$$2^{\text{qPCR cycle of no-antibody control DNA} - \text{qPCR cycle of enriched DNA}}$$

Enrichment of DNA fragments was normalized against an amplified control region using the control primers, located approximately 4 kb upstream of the ERR $\alpha$  transcriptional start site. Table S3 shows the specific mouse primers designed and used for ChIP qPCR analysis.

### Transfection Assays

See Supplemental Experimental Procedures for a description of the reporter constructs and expression plasmids used for transfections. Luciferase activity was measured 24 hr posttransfection, and results are shown in relative luciferase units.

### Electromobility Shift Assay, Coimmunoprecipitation, and Immunoblotting Assays

See Supplemental Experimental Procedures.

### Serial ChIP

An initial 10% input sample was kept for subsequent analysis. Following immunoprecipitation with either anti-ERR $\alpha$  or anti-ERR $\gamma$  antibody, enriched crosslinked genomic fragments from mouse heart tissue were eluted from the immunoprecipitate using two subsequent elutions with elution buffer (1% SDS, 0.1 M NaHCO<sub>3</sub>) by incubation at room temperature for 15 min. For each serial ChIP analysis, 10%

of the immunoprecipitated sample was decrosslinked in elution buffer by incubation at 65°C overnight, and the remaining 90% was reimmunoprecipitated with either anti-ERR $\alpha$  or anti-ERR $\gamma$  antibody. Quantification of ERR $\alpha$  and  $\gamma$  promoter occupancy was performed by calculating ERR enrichment relative to the initial 10% input sample. Amplification of ERR-enriched serial ChIP samples using a control region (~4 kb upstream of the *Esrra* promoter) served to calculate the overall background of the re-ChIP experiments.

### Computational Motif Discovery

De novo motif discovery was performed using MDScan (Liu et al., 2002) on the extended promoter regions of ERR $\alpha$ / $\gamma$  target genes (-1.5 kb to +0.5 kb from the TSS). The same regions were scanned for matches to TRANSFAC 7.2 position-weight matrices (PWMs) using a likelihood ratio approach based on a third-order Markov background model with locally determined GC content (Blanchette et al., 2006). Hits with p value below 10<sup>-4</sup> (on either strand) were predicted as putative binding sites. For each PWM, the total number of sites in the ERR extended promoters was compared to the number of such sites in the extended promoters of all genes in the mouse genome, and the site enrichment was assigned a p value based on a hypergeometric distribution. A similar calculation was performed separately for ERRE-containing promoters (i.e., those containing at least one predicted ERR site) and non-ERRE-containing promoters.

### Expression Profiling Analysis in Wild-Type versus ERR $\alpha$ Null Hearts

Triplicate microarray analyses of wild-type and ERR $\alpha$  null hearts were performed as described in Supplemental Experimental Procedures. A p value cutoff of  $\leq 0.001$  and a relative fold change (log<sub>2</sub>) cutoff of  $\pm 0.5$  were used, and genes were classified by biological function based on GO annotation (<http://fatigo.bioinfo.cipf.es/>) and NCBI gene descriptions. Relative fold expression levels of the analyzed genes using specific primers (Table S4) were normalized to *Actb* levels in the wild-type and ERR $\alpha$  null hearts.

### Expression Analysis in HL-1 Atrial Myocytes and Rat Neonatal Ventricular Myocytes

Quantitative real-time PCR was performed as described in Supplemental Experimental Procedures on RNA isolated from mouse HL-1 cardiomyocytes stably expressing GFP or a siERR $\gamma$ -encoding adenovirus following treatment for 24 hr with either 0.1% DMSO or the selective ERR $\alpha$  inverse agonist XCT790 (1  $\mu$ M), which is known to impair ERR $\alpha$ -mediated transcriptional activity (Willy et al., 2004). Experiments were performed in duplicate, and expression levels were normalized to *Arbp* levels. Similar experiments were performed with RNA isolated from rat neonatal ventricular myocytes expressing GFP, ERR $\alpha$ , or ERR $\gamma$  via adenoviral infection. Results were normalized against *Arbp* expression and reported relative to GFP (=1.0). Specific primers used are listed in Table S4.

### Immunofluorescence in Primary Ventricular Myocytes

See Supplemental Experimental Procedures.

### Supplemental Data

Supplemental Data include Supplemental Experimental Procedures, Supplemental References, five figures, and four tables and can be found with this article online at <http://www.cellmetabolism.org/cgi/content/full/5/5/345/DC1/>.

## ACKNOWLEDGMENTS

We thank C. Ouellet for mouse husbandry and G. Deblois, J. Laganière, A.-R. Bataille, and F. Robert for their contribution to the design of the genomic arrays and elaboration of protocols. W.A.A. was supported by the NIH Genetics Training Program. R.M.E. is the March of Dimes Chair in Molecular and Developmental Biology and an HHMI Investigator. This work was supported by grants from the Canadian

Institutes for Health Research and Genome Québec/Canada to V.G. and the NIH to R.M.E. (R01 HD27183), J.M.H. (K01 DK063051) and D.P.K. (R01 HL058493).

Received: November 10, 2006

Revised: February 16, 2007

Accepted: March 14, 2007

Published: May 8, 2007

## REFERENCES

- Abu-Elheiga, L., Brinkley, W.R., Zhong, L., Chirala, S.S., Woldegiorgis, G., and Wakil, S.J. (2000). The subcellular localization of acetyl-CoA carboxylase 2. *Proc. Natl. Acad. Sci. USA* *97*, 1444–1449.
- Abu-Elheiga, L., Matzuk, M.M., Abo-Hashema, K.A., and Wakil, S.J. (2001). Continuous fatty acid oxidation and reduced fat storage in mice lacking acetyl-CoA carboxylase 2. *Science* *291*, 2613–2616.
- Al-Shahrour, F., Diaz-Uriarte, R., and Dopazo, J. (2004). FatiGO: a web tool for finding significant associations of Gene Ontology terms with groups of genes. *Bioinformatics* *20*, 578–580.
- Araki, M., and Motojima, K. (2006). Identification of ERR $\alpha$  as a specific partner of PGC-1 $\alpha$  for the activation of PDK4 gene expression in muscle. *FEBS J.* *273*, 1669–1680.
- Barry, J.B., Laganière, J., and Giguère, V. (2006). A single nucleotide in an estrogen related receptor  $\alpha$  site can dictate mode of binding and PGC-1 $\alpha$  activation of target promoters. *Mol. Endocrinol.* *20*, 302–310.
- Blais, A., and Dynlacht, B.D. (2005). Constructing transcriptional regulatory networks. *Genes Dev.* *19*, 1499–1511.
- Blanchette, M., Bataille, A.R., Chen, X., Poitras, C., Laganière, J., Lefebvre, C., Deblois, G., Giguère, V., Ferretti, V., Bergeron, D., et al. (2006). Genome-wide computational prediction of transcriptional regulatory modules reveals new insights into human gene expression. *Genome Res.* *16*, 656–668.
- Bookout, A.L., Jeong, Y., Downes, M., Yu, R.T., Evans, R.M., and Mangelsdorf, D.J. (2006). Anatomical profiling of nuclear receptor expression reveals a hierarchical transcriptional network. *Cell* *126*, 789–799.
- Carroll, J.S., Liu, X.S., Brodsky, A.S., Li, W., Meyer, C.A., Szary, A.J., Eeckhoutte, J., Shao, W., Hestermann, E.V., Geistlinger, T.R., et al. (2005). Chromosome-wide mapping of estrogen receptor binding reveals long-range regulation requiring the forkhead protein FoxA1. *Cell* *122*, 33–43.
- Carroll, J.S., Meyer, C.A., Song, J., Li, W., Geistlinger, T.R., Eeckhoutte, J., Brodsky, A.S., Keeton, E.K., Fertuck, K.C., Hall, G.F., et al. (2006). Genome-wide analysis of estrogen receptor binding sites. *Nat. Genet.* *38*, 1289–1297.
- Cartoni, R., Leger, B., Hock, M.B., Praz, M., Crettenand, A., Pich, S., Ziltener, J.L., Luthi, F., Deriaz, O., Zorzano, A., et al. (2005). Mitofusins 1/2 and ERR $\alpha$  expression are increased in human skeletal muscle after physical exercise. *J. Physiol.* *567*, 349–358.
- Chao, E.Y., Collins, J.L., Gaillard, S., Miller, A.B., Wang, L., Orband-Miller, L.A., Nolte, R.T., McDonnell, D.P., Willson, T.M., and Zuercher, W.J. (2006). Structure-guided synthesis of tamoxifen analogs with improved selectivity for the orphan ERR $\gamma$ . *Bioorg. Med. Chem. Lett.* *16*, 821–824.
- Cheng, A.S., Jin, V.X., Fan, M., Smith, L.T., Liyanarachchi, S., Yan, P.S., Leu, Y.W., Chan, M.W., Plass, C., Nephew, K.P., et al. (2006). Combinatorial analysis of transcription factor partners reveals recruitment of c-MYC to estrogen receptor- $\alpha$  responsive promoters. *Mol. Cell* *21*, 393–404.
- Giguère, V. (1999). Orphan nuclear receptors: from gene to function. *Endocr. Rev.* *20*, 689–725.
- Giguère, V., Yang, N., Segui, P., and Evans, R.M. (1988). Identification of a new class of steroid hormone receptors. *Nature* *331*, 91–94.
- Hilfiker-Kleiner, D., Hilfiker, A., and Drexler, H. (2005). Many good reasons to have STAT3 in the heart. *Pharmacol. Ther.* *107*, 131–137.
- Hong, H., Yang, L., and Stallcup, M.R. (1999). Hormone-independent transcriptional activation and coactivator binding by novel orphan nuclear receptor ERR3. *J. Biol. Chem.* *274*, 22618–22626.
- Huss, J.M., and Kelly, D.P. (2004). Nuclear receptor signaling and cardiac energetics. *Circ. Res.* *95*, 568–578.
- Huss, J.M., Kopp, R.P., and Kelly, D.P. (2002). Peroxisome proliferator-activated receptor coactivator-1 $\alpha$  (PGC-1 $\alpha$ ) coactivates the cardiac-enriched nuclear receptors estrogen-related receptor- $\alpha$  and - $\gamma$ . Identification of novel leucine-rich interaction motif within PGC-1 $\alpha$ . *J. Biol. Chem.* *277*, 40265–40274.
- Huss, J.M., Pineda Torra, I., Staels, B., Giguère, V., and Kelly, D.P. (2004). Estrogen-related receptor  $\alpha$  directs peroxisome proliferator-activated receptor  $\alpha$  signaling in the transcriptional control of energy metabolism in cardiac and skeletal muscle. *Mol. Cell. Biol.* *24*, 9079–9091.
- Ichida, M., Nemoto, S., and Finkel, T. (2002). Identification of a specific molecular repressor of the peroxisome proliferator-activated receptor  $\gamma$  coactivator-1 $\alpha$  (PGC- $\alpha$ ). *J. Biol. Chem.* *277*, 50991–50995.
- Kahn, B.B., Alquier, T., Carling, D., and Hardie, D.G. (2005). AMP-activated protein kinase: ancient energy gauge provides clues to modern understanding of metabolism. *Cell Metab.* *1*, 15–25.
- Kamei, Y., Ohizumi, H., Fujitani, Y., Nemoto, T., Tanaka, T., Takahashi, N., Kawada, T., Miyoshi, M., Ezaki, O., and Kakizuka, A. (2003). PPAR $\gamma$  coactivator 1 $\beta$ /ERR ligand 1 is an ERR protein ligand, whose expression induces a high-energy expenditure and antagonizes obesity. *Proc. Natl. Acad. Sci. USA* *100*, 12378–12383.
- Laganière, J., Tremblay, G.B., Dufour, C.R., Giroux, S., Rousseau, F., and Giguère, V. (2004). A polymorphic autoregulatory hormone response element in the human estrogen related receptor  $\alpha$  (ERR $\alpha$ ) promoter dictates PGC-1 $\alpha$  control of ERR $\alpha$  expression. *J. Biol. Chem.* *279*, 18504–18510.
- Laganière, J., Deblois, G., Lefebvre, C., Bataille, A.R., Robert, F., and Giguère, V. (2005). Location analysis of estrogen receptor  $\alpha$  target promoters reveals that FOXA1 defines a domain of the estrogen response. *Proc. Natl. Acad. Sci. USA* *102*, 11651–11656.
- Lin, J., Puigserver, P., Donovan, J., Tarr, P., and Spiegelman, B.M. (2002). Peroxisome proliferator-activated receptor  $\gamma$  coactivator 1 $\beta$  (PGC-1 $\beta$ ), a novel PGC-1-related transcription coactivator associated with host cell factor. *J. Biol. Chem.* *277*, 1645–1648.
- Lin, J., Handschin, C., and Spiegelman, B.M. (2005). Metabolic control through the PGC-1 family of transcription coactivators. *Cell Metab.* *1*, 361–370.
- Liu, X.S., Brutlag, D.L., and Liu, J.S. (2002). An algorithm for finding protein DNA binding sites with applications to chromatin-immunoprecipitation microarray experiments. *Nat. Biotechnol.* *20*, 835–839.
- Luo, J., Sladek, R., Carrier, J., Bader, J.-A., Richard, D., and Giguère, V. (2003). Reduced fat mass in mice lacking orphan nuclear receptor estrogen-related receptor  $\alpha$ . *Mol. Cell. Biol.* *23*, 7947–7956.
- Mark, M., Ghyselinck, N.B., and Chambon, P. (2006). Function of retinoid nuclear receptors: lessons from genetic and pharmacological dissections of the retinoic acid signaling pathway during mouse embryogenesis. *Annu. Rev. Pharmacol. Toxicol.* *46*, 451–480.
- Mootha, V.K., Handschin, C., Arlow, D., Xie, X., St Pierre, J., Sihag, S., Yang, W., Altshuler, D., Puigserver, P., Patterson, N., et al. (2004). ERR $\alpha$  and GABPA $\alpha/\beta$  specify PGC-1 $\alpha$ -dependent oxidative phosphorylation gene expression that is altered in diabetic muscle. *Proc. Natl. Acad. Sci. USA* *101*, 6570–6575.
- Odom, D.T., Zizlsperger, N., Gordon, D.B., Bell, G.W., Rinaldi, N.J., Murray, H.L., Volkert, T.L., Schreiber, J., Rolfe, P.A., Gifford, D.K., et al. (2004). Control of pancreas and liver gene expression by HNF transcription factors. *Science* *303*, 1378–1381.
- Olson, E.N. (2006). Gene regulatory networks in the evolution and development of the heart. *Science* *313*, 1922–1927.

- Puigserver, P., Wu, Z., Park, C.W., Graves, R., Wright, M., and Spiegelman, B.M. (1998). A cold-inducible coactivator of nuclear receptors linked to adaptive thermogenesis. *Cell* 92, 829–839.
- Scarpulla, R.C. (2006). Nuclear control of respiratory gene expression in mammalian cells. *J. Cell. Biochem.* 97, 673–683.
- Schreiber, S.N., Knutti, D., Brogli, K., Uhlmann, T., and Kralli, A. (2003). The transcriptional coactivator PGC-1 regulates the expression and activity of the orphan nuclear receptor ERR $\alpha$ . *J. Biol. Chem.* 278, 9013–9018.
- Schreiber, S.N., Emter, R., Hock, M.B., Knutti, D., Cardenas, J., Podvinec, M., Oakeley, E.J., and Kralli, A. (2004). The estrogen-related receptor alpha (ERR $\alpha$ ) functions in PPAR $\gamma$  coactivator 1 $\alpha$  (PGC-1 $\alpha$ )-induced mitochondrial biogenesis. *Proc. Natl. Acad. Sci. USA* 101, 6472–6477.
- Sladek, R., Bader, J.-A., and Giguère, V. (1997). The orphan nuclear receptor estrogen-related receptor  $\alpha$  is a transcriptional regulator of the human medium-chain acyl coenzyme A dehydrogenase gene. *Mol. Cell. Biol.* 17, 5400–5409.
- Taegtmeyer, H., Golfman, L., Sharma, S., Razeghi, P., and van Arsdall, M. (2004). Linking gene expression to function: metabolic flexibility in the normal and diseased heart. *Ann. N Y Acad. Sci.* 1015, 202–213.
- Vega, R.B., and Kelly, D.P. (1997). A role for estrogen-related receptor  $\alpha$  in the control of mitochondrial fatty acid  $\beta$ -oxidation during brown adipocyte differentiation. *J. Biol. Chem.* 272, 31693–31699.
- Wende, A.R., Huss, J.M., Schaeffer, P.J., Giguère, V., and Kelly, D.P. (2005). PGC-1 $\alpha$  coactivates PDK4 gene expression via the orphan nuclear receptor ERR $\alpha$ : a mechanism for transcriptional control of muscle glucose metabolism. *Mol. Cell. Biol.* 25, 10684–10694.
- Willy, P.J., Murray, I.R., Qian, J., Busch, B.B., Stevens, W.C., Jr., Martin, R., Mohan, R., Zhou, S., Ordentlich, P., Wei, P., et al. (2004). Regulation of PPAR $\gamma$  coactivator 1 $\alpha$  (PGC-1 $\alpha$ ) signaling by an estrogen-related receptor  $\alpha$  (ERR $\alpha$ ) ligand. *Proc. Natl. Acad. Sci. USA* 101, 8912–8917.
- Zhang, X., Odom, D.T., Koo, S.H., Conkright, M.D., Canettieri, G., Best, J., Chen, H., Jenner, R., Herbolsheimer, E., Jacobsen, E., et al. (2005). Genome-wide analysis of cAMP-response element binding protein occupancy, phosphorylation, and target gene activation in human tissues. *Proc. Natl. Acad. Sci. USA* 102, 4459–4464.

#### Accession Numbers

The expression data discussed in this publication have been deposited in the NCBI Gene Expression Omnibus (<http://www.ncbi.nlm.nih.gov/geo/>) under the GEO series accession number GSE7196.